Solar Energy Materials & Solar Cells 96 (2012) 231–237

Contents lists available at SciVerse ScienceDirect

Solar Energy Materials & Solar Cells

journal homepage: www.elsevier.com/locate/solmat

Quantitative assessment of optical losses in thin-film CdS/CdTe solar cells

L.A. Kosyachenko [a,*], E.V. Grushko [a], X. Mathew [b]

[a] Chernivtsi National University, 58012 Chernivtsi, Ukraine
[b] Centro de Investigacion en Energia, Universidad Nacional Autonoma de Mexico, Temixco, Morelos 62580, México

ARTICLE INFO

Article history:
Received 27 June 2011
Received in revised form
20 September 2011
Accepted 29 September 2011
Available online 19 October 2011

Keywords:
CdS/CdTe solar cells
Optical constant
Optical losses

ABSTRACT

For the first time, based on the known optical constants of the materials (refractive index and extinction coefficient), calculations of optical losses in glass/transparent conducting oxide (TCO)/CdS/CdTe solar cells have been carried out taking into account reflections at the interfaces and absorption in the TCO (it can be indium tin oxide (ITO) or SnO_2:F) and CdS layers. It has been shown that the losses caused by reflections at the interfaces result in lowering the short-circuit current by ~9 % whereas absorption in the TCO and CdS layers with the typical thicknesses lead to losses of 15–16% for glass/SnO_2/CdS/CdTe, and 22–24% for glass/ITO/CdS/CdTe solar cells. At 100% photoelectric conversion in the CdTe absorber layer, this corresponds to a loss in short-circuit current by ~3 mA/cm^2 due to reflection, and 4–7 mA/cm^2 due to absorption at the glass/SnO_2(or ITO)/CdS stack. Losses due to absorption in float glass and low-iron glasses are 3.3–3.5% and 0.6–0.7%, respectively.

1. Introduction

Since the beginning of the last decade mass production of solar modules based on thin-film CdS/CdTe has been started. In 2009–2010, annual production capacity of such devices by one company, First Solar, exceeded 1 GW and in 2011 it is expected to double the production [1]. It is considered that the rapid development of this solar energy technology sector is mainly due to the lower cost of CdTe modules compared to those based on Si wafers. Today the challenge facing the researchers and technologists is how to increase the efficiency of CdS/CdTe modules from the current large area efficiency of 10–11% and decrease the gap between actual efficiency and the theoretical limit of 28–30% [2–4]. The main causes of efficiency loss in CdTe/CdS solar cells are optical, electrical and recombination, a topic of study discussed in a substantial amount of papers. In the literature there are a good amount of experimental data on the optical transmission of the glass/ITO(or SnO_2) and glass/ITO(or SnO_2)/CdS structures that provide information about the losses caused by reflection from the interfaces and absorption in the ITO, SnO_2 and CdS layers (ITO is a solid solution of indium oxide (In_2O_3) and tin oxide (SnO_2)) [5–7]. However, in the first case, the surface of ITO (or SnO_2) layer is in optical contact with air, rather than with CdS, as in the real case. In the second case, the surface of CdS is in contact with air rather with the CdTe layer. As discussed in this paper, measuring the transmission of the glass/ITO (or SnO_2) and glass/ITO (or SnO_2)/CdS structures leads to the results, which differ significantly from those measured on the real structure of the solar cell. Due to the large differences in refractive indices and extinction coefficients between air and other device layers such as ITO, SnO_2 and CdS, the reflection coefficient at the interfaces measured and reported can be higher than that in the case of the real structure. Further, in the literature, pronounced interference oscillations in the transmission curves are always observed, which are relatively stronger than in the real device structure (as follows from the calculation results discussed here). To our knowledge, the studies of optical losses in CdTe/CdS solar cells based on optical constants of materials used, i.e. based on general principles, are absent in the literature. The present study focuses on optical losses due to absorption and reflection at the interfaces in CdTe/CdS solar cells. Calculations have been carried out based on the optical constants of materials used, the refractive index and extinction coefficient. It seems that the results of these calculations are interesting from a scientific and practical point of view, since they suggest possible ways to increase the efficiency of CdTe/CdS solar cells by reducing the optical losses, and vice versa they show the efforts that are not justified if a decrease in the optical losses gives only a small gain.

2. Reflection losses

The sketch of a typical glass/TCO/CdS/CdTe solar cell is shown in Fig. 1 (TCO refers to a transparent conducting oxide). Before reaching the photoelectrically active CdTe absorber layer, solar radiation penetrates the glass plate, a TCO layer and a CdS

* Corresponding author.
E-mail address: l.a.kosyachenko@gmail.com (L.A. Kosyachenko).

0927-0248/$ - see front matter © 2011 Elsevier B.V. All rights reserved.
doi:10.1016/j.solmat.2011.09.063

window layer. Obviously, this is accompanied by optical losses upon reflection from the following interfaces: air–glass, glass–TCO, TCO–CdS and CdS–CdTe, and absorption in glass plate, TCO and CdS. According to the Fresnel equations, when the light is at near-normal incidence, the reflection coefficient (reflectivity) from the interface between two contacting materials is determined by their refractive indices n_1 and n_2

$$R=\left(\frac{n_1-n_2}{n_1+n_2}\right)^2 \tag{1}$$

In the case of electrically conductive materials, the refractive index contains an imaginary part and is written as $n^*=n-i\kappa$, where n is the refractive index, and κ is the extinction coefficient ($i=\sqrt{-1}$). The reflection coefficient from the interface is defined as the square of the modulus $[(n_1^*-n_2^*)/(n_1^*+n_2^*)]$ [8] and has the form:

$$R=\frac{|n_1^*-n_2^*|^2}{|n_1^*+n_2^*|^2}=\frac{(n_1-n_2)^2+(\kappa_1-\kappa_2)^2}{(n_1+n_2)^2+(\kappa_1+\kappa_2)^2} \tag{2}$$

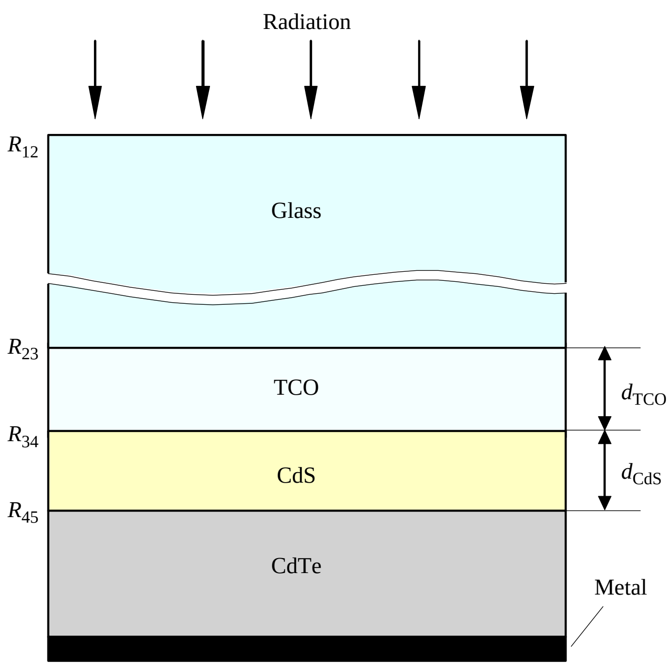

Fig. 1. Schematic cross-section of thin-film CdS/CdTe solar cell.

At the air–glass interface (see Fig. 1) we will find the reflection coefficient R_{12} taking $n_1=1$, and $\kappa_1=0$ for the air. For the convenience of presenting the main optical losses, we first assume that for glass $\kappa_2=0$. This is justified by the fact that photovoltaic applications often use specialized glass with low iron oxide content, where the absorption is observed only in the ultraviolet region. As it will be shown later, absorption in the low-iron glass practically does not exhibit itself in short-circuit current, however, in the case of ordinary glass (float glass) absorption losses become noticeable.

For the refractive index of glass n_1 we will use the Sellmeier (Zelmeer) dispersion equation applied for quartz (SiO_2) [9]:

$$n^2=1+\frac{a_1\lambda^2}{\lambda^2-\lambda_1^2}+\frac{a_2\lambda^2}{\lambda^2-\lambda_2^2}+\frac{a_3\lambda^2}{\lambda^2-\lambda_3^2} \tag{3}$$

where $a_1=0.6962$, $a_2=0.4079$, $a_3=0.8974$, $\lambda_1=68$ nm, $\lambda_2=116$ nm and $\lambda_3=9896$ nm.

To find the reflection coefficients at the interfaces: glass–TCO, TCO–CdS and CdS–CdTe it is necessary to know the values of the refractive index and extinction coefficient of TCO, CdS and CdTe in the spectral range 300–850 nm. In the discussion below we consider the two most common structures of CdTe/CdS solar cell in which indium tin oxide (ITO) and F-doped tin oxide (SnO_2:F) are used as TCO. Fig. 2 shows the spectral dependences of n and κ for ITO (typically 90% In_2O_3, 10% SnO_2) taken from Refs. [10,11] and for SnO_2:F taken from Ref. [12]. Also shown are data on CdS [13] and CdTe [14].

Note that the data on the optical constants of the materials cited in various sources differ somewhat, depending on the method adopted to grow the crystal or film. However, with a few exceptions, these differences manifest themselves weakly in the results of the calculation of the integral characteristics of a multilayer solar cell, which is short-circuit current J_{sc}. For example, calculations of J_{sc} using data for n and κ, obtained by ellipsometry for CdTe single crystal and films [14], lead to almost identical results.

Fig. 3 shows the spectral dependence of the reflection coefficients $R(\lambda)$ at the interfaces calculated by substituting n and κ

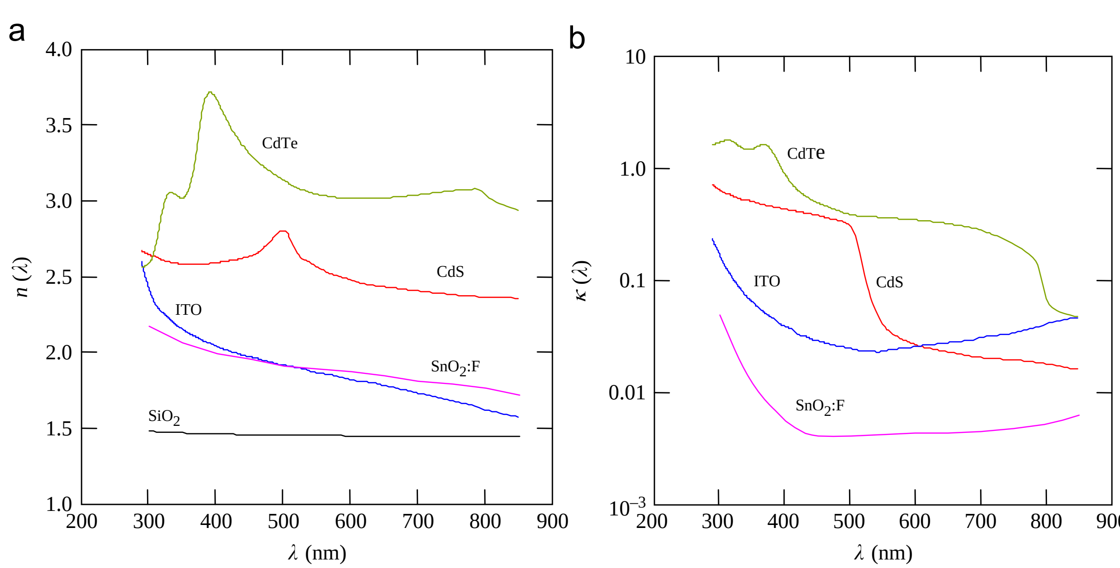

Fig. 2. Refractive index (a), and extinction coefficient (b) of SiO_2, ITO, SnO_2:F, CdS and CdTe as a function of wavelength (the curves $\kappa(\lambda)$ for glasses are shown in Fig. 7(b)).

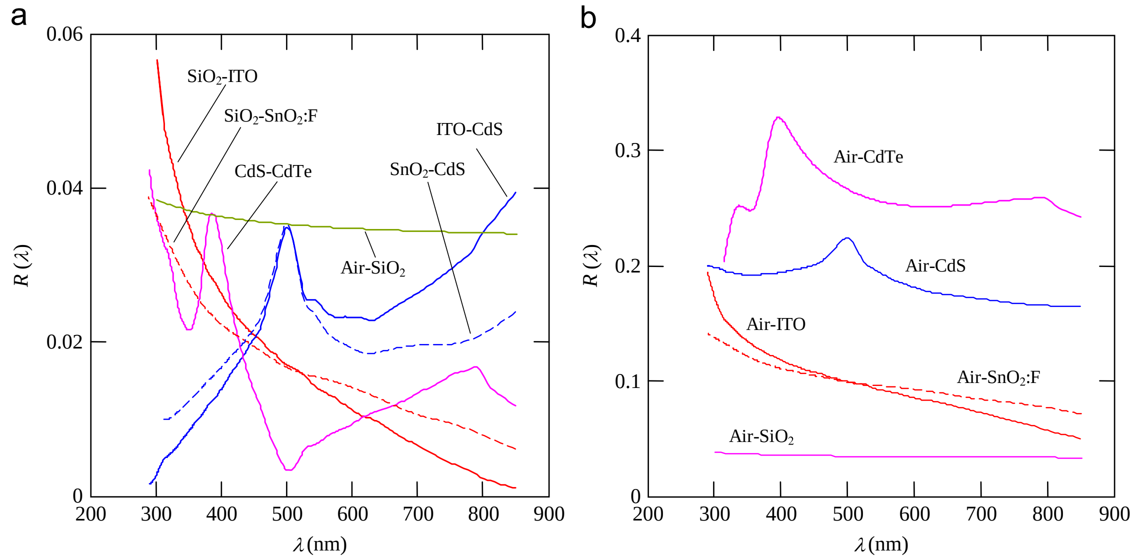

Fig. 3. Reflection coefficients R for the interfaces: air–glass (SiO_2), glass–ITO, glass–SnO_2, SnO_2–CdS, CdS–CdTe (a); and air–ITO, air–CdS, air–CdTe (b).

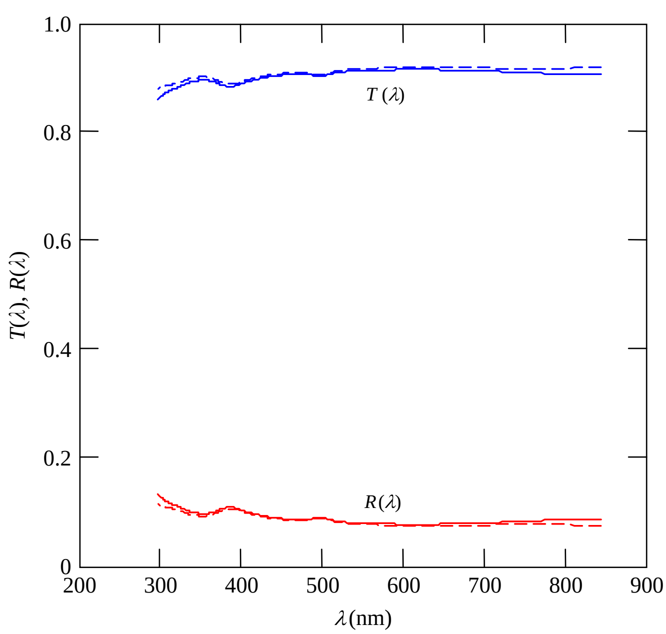

Fig. 4. Calculated transmittance $T(\lambda)$ and reflectance $R(\lambda)$ of the glass/ITO/CdS (solid line) and glass/SnO_2/CdS (dashed line) structures considering only reflections from all interfaces.

from Fig. 2 into Eq. (2). Emphasis is given on obtaining low reflection coefficients (less than 0.05–0.06). The explanation for this is a relatively small difference between the optical constants of contacting materials. The calculation results shown in Fig. 3(b) for reflection at the interfaces of the same materials (shown in Fig. 3(a)) with air give the usually observed values of R: 0.037–0.034 for the air/glass interface, 0.25–0.35 for the air/CdTe interface, etc.

As a consequence of the conservation of energy, the transmission coefficient (transmission) in each interface is given by $T=1-R$. Therefore, for reflection losses at all interfaces before the solar radiation reaches the CdTe absorber layer (Fig. 4), the transmission $T(\lambda)$ can be calculated by the formula:

$$T(\lambda)=(1-R_{12})(1-R_{23})(1-R_{34})(1-R_{45}) \tag{4}$$

where R_{12}, R_{23}, R_{34} and R_{45} are the reflection coefficients of the interfaces: air–glass, glass–ITO (or glass–SnO2), ITO–CdS (or SnO_2–CdS), and CdS–CdTe, respectively (see Fig. 1). We consider normal incidence of the rays. As will be explained below, the multiple reflections of rays have a negligible impact due to the relatively close values of the refractive indices of the contacting materials.

It follows from Fig. 4 that the total reflection losses at the interfaces: air–glass, glass–ITO, ITO–CdS and CdS–CdTe in the thin-film CdS/CdTe solar cell is about 9% in the entire spectral range 300–850 nm. This implies that the reflection losses in the case of thin-film CdS/CdTe structure are not as critical as in the case of a silicon solar cell. In fact, the coefficient of reflection from the mirror surface of silicon is at least 30%, while in the region $\lambda<400$ nm they are even higher than 50%.

Eq. (4) does not account for multiple reflections in the glass plate, ITO and CdS layers, which is quite acceptable because of the small difference of reflection coefficients at the interfaces (Fig. 3(a)). Accounting for multiple reflections only complicates the expression for the transmission but leads to the results virtually identical to those shown in Fig. 4. Estimates of the errors, which are the results of neglecting multiple reflections and related interference, are discussed in Section 4 below in the calculation of the short-circuit current density.

3. Absorption losses

The data for the extinction coefficient $\kappa(\lambda)$ shown in Fig. 2(b) allows to find the absorption coefficient:

$$\alpha(\lambda)=\frac{2\omega}{c}\kappa=\frac{4\pi}{\lambda}\kappa \tag{5}$$

where $\omega=2\pi\nu$ is the angular frequency, and c is the speed of light in free space.

Knowing $\alpha(\lambda)$ for the CdS and ITO (SnO_2), the absorption in these layers can be taken into account by incorporating in Eq. (4) the addition factors $\exp[-\alpha_{CdS}(\lambda)d_{CdS}]$, $\exp[-\alpha_{ITO}(\lambda)d_{ITO}]$ and $\exp[-\alpha_{SnO}(\lambda)d_{SnO}]$:

$$T(\lambda)=(1-R_{12})(1-R_{23})(1-R_{34})(1-R_{45})\exp(-\alpha_{ISnO}d_{SnO})\exp(-\alpha_{CdS}d_{CdS}) \tag{6}$$

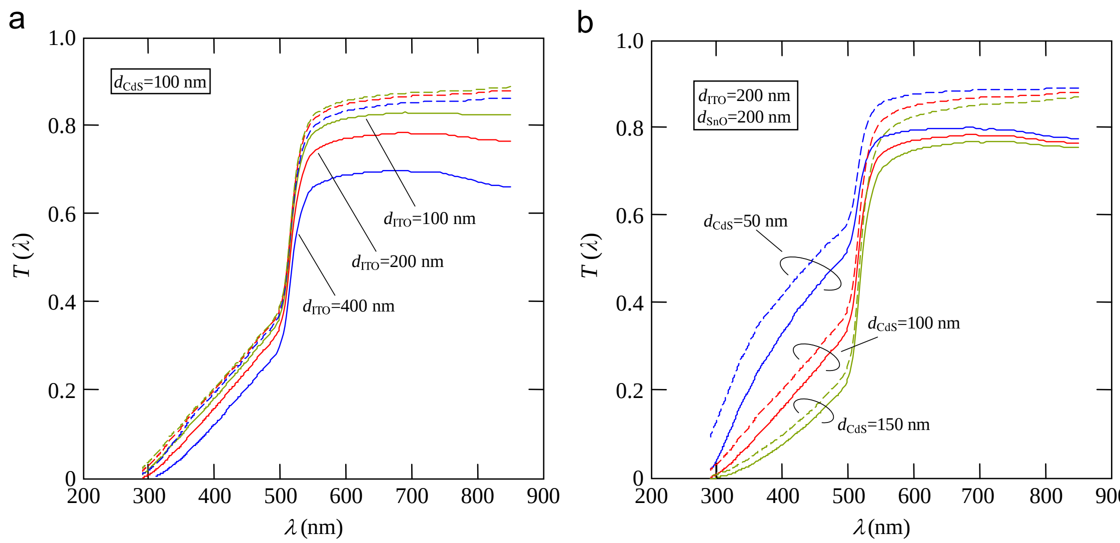

Fig. 5. Transmission of the glass/ITO/CdS (solid lines) and glass/SnO_2/CdS (dashed lines) structures calculated (a) at $d_{CdS}=100$ nm and different thicknesses of ITO and SnO_2:F and (b) at $d_{ITO}=d_{SnO}=200$ nm and different thicknesses of the CdS layer.

or

$$T(\lambda)=(1-R_{12})(1-R_{23})(1-R_{34})(1-R_{45})\exp(-\alpha_{ITO}d_{ITO})\exp(-\alpha_{CdS}d_{CdS}) \quad (7)$$

where d_{ITO} and d_{CdS} are the thicknesses of the ITO and CdS layers, respectively.

Fig. 5 shows the transmission of the glass/ITO/CdS structure (solid lines) and the glass/SnO_2/CdS structure (dashed lines) calculated with various thicknesses of the ITO, SnO_2:F and CdS layers.

As can be seen from Fig. 5, appreciable losses (10–15%) are observed in the wavelength range $\lambda > 500$–550 nm caused by absorption in SnO_2:F and greater losses (15–35%) in the case of ITO (in addition to reflection). Much more losses are observed in the region $\lambda < 500$–550 nm caused by absorption in CdS together with ITO or SnO_2:F. In the wavelength region $\lambda > 500$–550 nm, by thinning the ITO it is possible to reduce the optical losses by 12–15%; however, the effect of SnO_2:F thickness is only nominal. Greater effect can be achieved in the $\lambda < 500$–550 nm range by decreasing the thickness of the CdS layer. It is known, however, that it is difficult to obtain uniform and pin-hole free CdS layers thinner than ~50 nm.

4. Effect of absorption in ITO and CdS layers on short-circuit current

Calculation of short circuit current can quantitatively account for the effect of optical losses in the whole spectral range. We will calculate the short-circuit current density J_{sc} for AM1.5 total solar radiation using the Table ISO 9845-1:1992 [15].

If Φ_i is the spectral radiation power density and $h\nu$ is the photon energy, and the spectral density of the incident photon flux is $\Phi_i/h\nu_i$, then we can write J_{sc} as

$$J_{sc}=q\sum_i T(\lambda)\frac{\Phi_i(\lambda)}{h\nu_i}\Delta\lambda_i \quad (8)$$

where $\Delta\lambda_i$ is the wavelength range between the neighboring values of λ_i (the photon energy $h\nu_i$) in the table and the summation is over the spectral range $\lambda=300$ nm to $\lambda=\lambda_g=hc/E_g\approx 840$ nm.

Fig. 6(a) shows the dependence of short circuit current J_{sc} on the thickness of ITO and SnO2:F calculated for different thickness of CdS with the assumption that the efficiency of photoelectric conversion in the CdTe layer is equal to 100%.

Fig. 6(b) shows the percentage decreases of the short circuit current due to the reflection of solar radiation from the interfaces and absorption in the layers ITO (or SnO_2:F) and CdS. In this case, the value of the optical losses ξ is found using the expression:

$$\xi=\left(1-\frac{J_{sc}}{J_{sc}^{o}}\right)100\% \quad (9)$$

where J_{sc}^{o} is the short-circuit current density found by Eq. (9) at $T(\lambda)=1$ ($J_{sc}^{o}=29.7$ mA/cm^2 according to the Table ISO 9845-1:1992).

As can be seen from Fig. 6, optical losses caused by TCO layer with thickness of 200 nm are about 20% and 10% for ITO and SnO_2:F, respectively. When the thickness of the TCO layer is close to 0, the optical losses are caused only by reflection and become equal to 8.5% and 8.8% for the SnO_2:F and ITO layers, respectively. Thicker ITO layers of 500–700 nm leads to unacceptably high optical losses (~40% at $d_{CdS}=0$), while using SnO_2:F the losses are only in the range of ~15% (at $d_{CdS}=0$). In both cases, the presence of CdS layer, even when its thickness is 50 nm leads to an additional increase in the optical losses by approximately 10% and when the CdS thickness is 100 nm, this additional loss is ~12% and 17%, respectively, for ITO and SnO_2. It should be borne in mind that the thickness of CdS equal to 50–60 nm is close to the minimum possible value with the current technology used in the manufacture of CdS/CdTe solar cells [16]. In the case of SnO_2:F transparent electrode, the presence of very thin CdS layer limits the short circuit current density J_{sc} at ~23 mA/cm^2, and the achievement of this value in ITO/CdS/CdTe solar cell is possible only with an ultra-thin ITO layer.

As is evident from the data obtained, a short-circuit current density above ~25 mA/cm^2 is practically impossible with the use of pure CdS as the window layer since the band gap is only 2.42 eV. However, slightly higher current ($J_{sc}\approx 26$ mA/cm^2) can be obtained with the use of modified CdS films with higher band gap. In TCO/Zn_2SnO_4/CdS/CdTe devices, for example, inter-diffusion between the CdS and Zn_2SnO_4 (ZTO) films effectively "consumes" relatively thick CdS film during device fabrication [17,18]. Another option for improving the charge collection in the short-wavelength region is the use of a wider band gap $Cd_{1-x}Zn_xS$ ternary alloy to replace CdS as the window layer [19]. Results of the calculations show that integrating a ZTO buffer layer into a

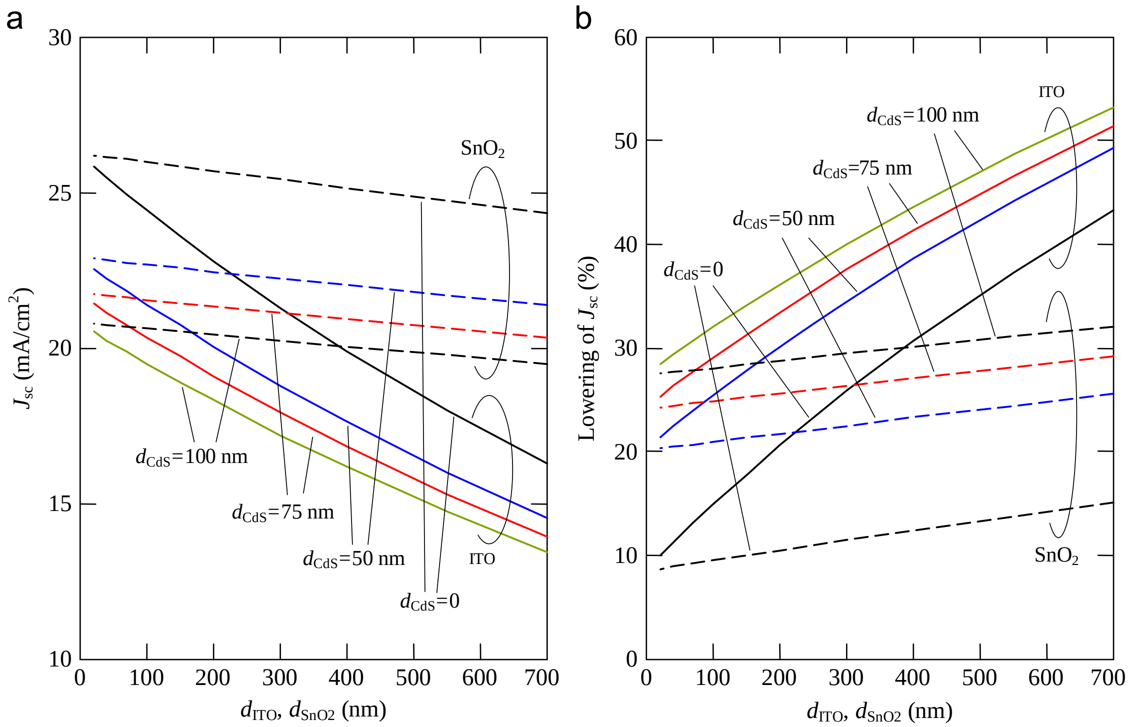

Fig. 6. (a) Effect of optical losses on short-circuit current depending on the thickness of ITO and SnO_2:F layer calculated for different thicknesses of CdS layer (100-percent photoelectric conversion efficiency for the CdTe absorber layer is assumed); (b) the same but expressed in percents.

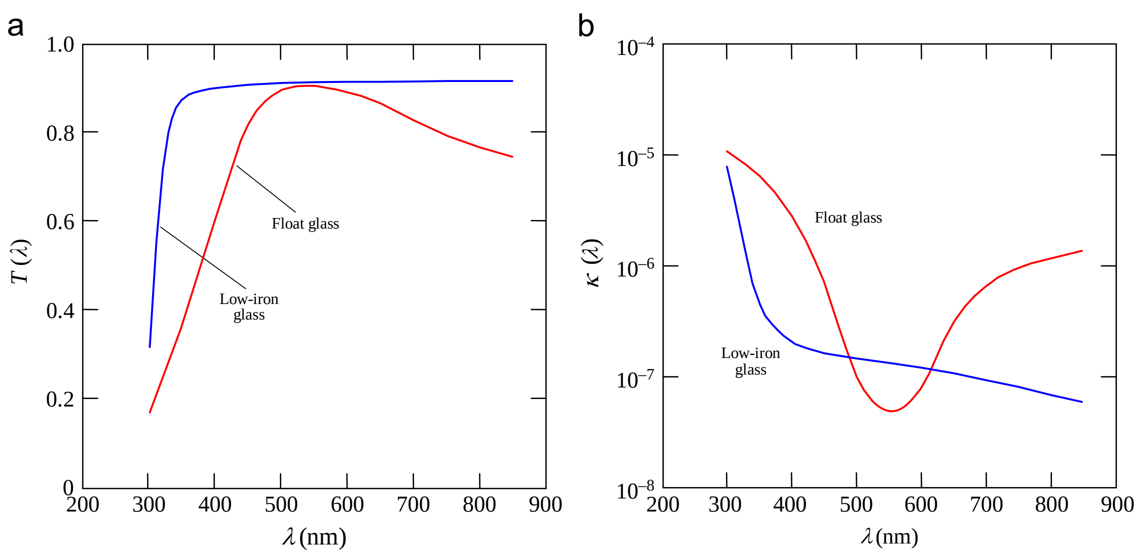

Fig. 7. Transmissions of (a) float glass, and (b) low iron glass.

CdTe cell with the intention of modifying the TCO layer (rather than CdS) results in a very insignificant increase in J_{sc}, since the optical losses in the TCO are mainly due to reflection rather than absorption. Remember that the indicated values of J_{sc} correspond to 100-percent photoelectric conversion efficiency for the CdTe absorber layer.

Considering the optical losses in a CdS/CdTe solar cell due to the light absorption in the glass substrate, as already mentioned, most glasses contain iron impurities in the form of iron salts within the silicon oxide that impede the transmission of light through the material. Because of this, in common glasses apart from a fairly strong absorption in the UV region, there is also a noticeable absorption in the visible and infrared regions. Specialized glasses with greater transmittance than ordinary soda lime glasses (window glass) are available in the market. These are glasses with low iron oxide content, i.e. the so-called low-iron solar glass with the virtual absence of color. Fig. 7(a) shows for example the curves of the optical transmission of ordinary float glass used for windows and low-iron glass produced by Targray Technology International Inc. for PV modules [20].

Knowing the transmission of the glass $T(\lambda)$, one can find the spectral dependence of its absorption coefficient $\alpha_{glass}(\lambda)$, using a formula that takes into account multiple reflections from the surfaces of the plate (by solving the equation for the transmission for this case [21]):

$$\alpha_{glass} = -\frac{1}{d_{glass}} \ln\left\{ \frac{1}{R_{12}{}^2} \left[-\frac{(1-R_{12})^2}{2T(\lambda)} + \left[\frac{(1-R_{12})^4}{4T(\lambda)^2} + R_{12}{}^2 \right]^{1/2} \right] \right\} \tag{10}$$

where d_{glass} is the glass thickness and R_{12} is the reflection coefficient at the air–glass interface.

The absorption coefficient α_{glass} is uniquely associated with the extinction coefficient κ_{glass} by the relation $\alpha_{glass}=(2\omega/c)\kappa_{glass}=(4\pi/\lambda)\kappa_{glass}$, using this one can find κ_{glass}. The obtained spectral dependences of float glass and low-iron solar glass are shown in Fig. 7(b). As can be seen, the extinction coefficients of both types of glasses are lower by several orders than those for ITO, SnO_2, CdS and CdTe (see Fig. 2(b)). But one should keep in mind that the thickness of the glass in the CdS/CdTe solar cell is at least three orders of magnitude greater than that of the thin-film device components.

To account for the absorption of glass in the calculation of short-circuit current density in the expressions for the transmissions (Eqs. (6) and (7)) it is obvious to introduce a factor $\exp[-\alpha_{glass}(\lambda)d_{glass}]$. Results of the calculations of short-circuit current density taking into account all the optical losses, including absorption in the 3 mm thick glass (with thickness of CdS layer 75 nm) are shown in Fig. 8. The solid, doted and dashed lines correspond, respectively, to glass with no absorption losses, low-iron glass and float glass. It follows from Fig. 8 that the absorption in the low-iron glass and the float glass reduces the short circuit current density J_{sc} by 0.6–0.7% and 3.3–3.5%, respectively. This corresponds to a decrease in the value of J_{sc} by 0.1–0.13 and 0.5–0.7 mA/cm^2, respectively, at a thickness of 500 μm for ITO or SnO_2 and assuming 100-percent light-to-electric conversion in the CdTe layer. Thus, optical losses due to absorption in the low-iron glass (0.6–0.7%) can be ignored without introducing appreciable error that was made in the above calculations. However, considering the fact that low-iron glass is expensive than float glass, a loss in J_{sc} of 0.5–0.7 mA/cm^2 with float glass can be acceptable in PV industry. Further, as seen from Fig. 3, the reflection coefficient R_{12} is very weakly depend on λ averaging about 3.5% and the contribution of the extinction coefficient ($\kappa=10^{-7}-10^{-5}$) to R_{12} is negligible according to Eq. (2) (see Fig. 7(b)). Therefore, we can right away say that the application of anti-reflective coating on the front surface of the glass can result in the ideal case an increase in the short-circuit density of ~3.5%, which corresponds to ~0.5 mA/cm^2.

Finally, considering the errors caused by neglecting the multiple reflections and the interference effects in the TCO and CdS layers, we estimate these effects using a somewhat simplified model, but, nevertheless, justify the lack of interference oscillations in the calculated transmission curves. As is known, the transmission of a transparent film of thickness d with refractive index n at normal incidence taking into account the interference is given by the equation widely known in optics as the Airy formula for multiple beam interference in a system of two parallel plane reflecting surfaces for the case of no absorption [22]

$$T(\lambda) = \frac{(1-R)^2}{(1-R)^2 + 4R\sin^2(4\pi nd/\lambda)} \tag{11}$$

where R is the reflection coefficient of the film surface.

In Eq. (11), it is assumed that the film is in contact with identical materials at both sides. From our point of view, interference effects appear considerably weaker if the film is in contact with materials having refractive index higher than that of air.

This is easily seen by considering multi-beam interference in a sheet layer of material when the layers on both sides are air and a different material. As an example, the calculation results obtained by Eq. (11) for the transmission of ITO layer, when it is in contact with air (solid oscillating line) and is in contact with SiO_2 (dashed oscillating line) are shown in Fig. 9. As can be seen, a pronounced oscillating interference behavior of $T(\lambda)$ is observed in both cases. However, as expected, in the case of reflection from ITO/SiO_2 interface, the amplitude of the oscillation is 5–7 times smaller, which is explained by a smaller difference in the refractive index and extinction coefficient at the interface.

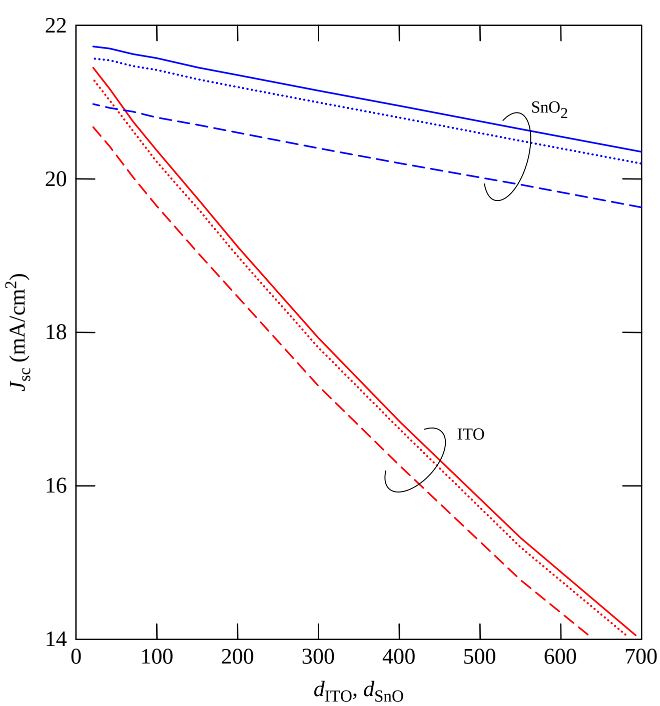

Fig. 8. Effect of absorption of glass substrate on short-circuit current density depending on thicknesses of ITO and SnO_2:F layers (the thickness of CdS layer is 75 nm). The solid, dotted and dashed lines show the calculated results respectively to glass with no absorption losses, low-iron glass and float glass.

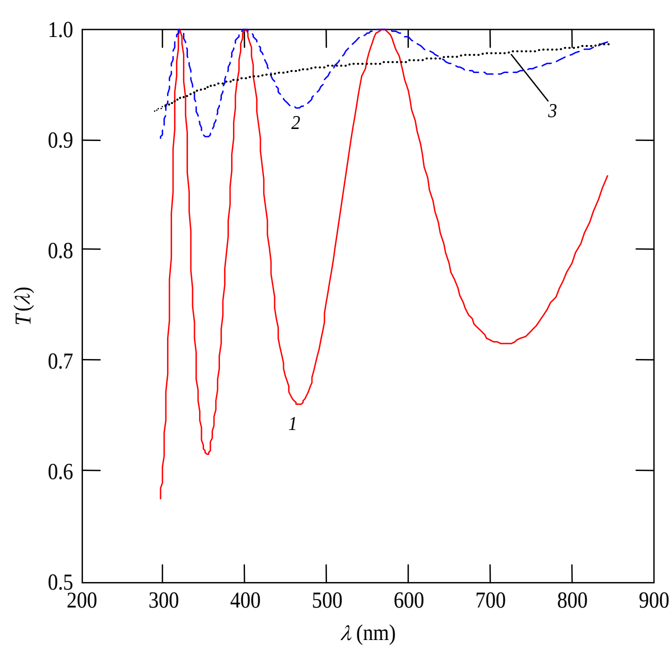

Fig. 9. Transmittance of the ITO film (d=200 nm) *in air* calculated by Eq. (11) (oscillating solid line 1), contacted from both sides with SiO_2 and calculated by Eq. (11) at $R=R_{23}$ (oscillating dashed line 2), and the same but calculated as $[1-R_{23}(\lambda)]^2$ (monotonically varying dotted line 3).

In Fig. 9, transmission of the ITO layer (dotted line 3, without oscillation) is calculated as $T(\lambda)=(1-R_{23})^2$, i.e. without taking into account multiple reflections. As one can see, the average transmission of the ITO film (dotted line 3) in optical contact with SiO_2 calculated using Eq. (11) and the curve $T(\lambda)=(1-R_{23})^2$ are comparable in magnitude. It can be assumed that short-circuit current density J_{sc}, as an *integrated* characteristic calculated over a broad spectral range, may vary slightly in these two cases. Interference oscillations in the transmission curves of the multilayer glass/ITO (or SnO_2) and glass/ITO (or SnO_2)/CdS structures are expressed even weaker than on the curve 2, shown by dashed line, since the positions of maxima and minima for the layers with different thicknesses and with different refractive indices do not coincide. Thus, the interference effects in the solar cells under study appear rather weak, i.e. they contribute only a minor error in the results of the calculation of short circuit current.

5. Conclusions

The results of the calculations performed in this study reveal the specific causes of the optical losses in the CdS/CdTe solar cell and the possibilities to reduce them.

(i) Reflection losses is about 8% over a wide spectral range, and only in the region $\lambda < 400$ nm (where the Sun radiation is weak in terrestrial conditions) increase to 10–11%. Certainly, reflection losses can be reduced by $\sim$ 4% using antireflection coating on the front surface of the glass. Since the reflection coefficient is determined by the difference between the optical constants of contacting materials, reflection losses in solar cells with ITO and SnO_2:F transparent electrodes differ very little.

(ii) ITO layer absorbs radiation much more than SnO_2:F layer. Due to absorption in the ITO layer of 200 nm thickness, the short-circuit current decreases by 12%, however, the decrease can be 25–26% when the thickness is 500 nm. In contrast, absorption in the SnO_2:F layer is much less, causing only a decrease in short circuit current of about 2% at a thickness of 200 nm, and 4–5% at a thickness of 500 nm (absorption in the SnO_2:F layer can be neglected when the thickness is in the range of 100 nm).

(iii) Absorption loss in CdS cannot be avoided by reducing thickness alone, since it is related to interband optical transitions. Even at a thickness of 50 nm, decrease in the short-circuit current, caused by absorption in the CdS layer, is about 10% and further increase of 5–6% occurs at a thickness of 100 nm. A solution to reduce the absorption loss in CdS is the modification of CdS layer with the interdiffusion between a special sub-layer and CdS or replacing CdS by a wide band gap semiconductor.

(iv) Absorption in the low-iron glass and the ordinary float glass reduces the short circuit current density by 0.6–0.7% and 3.3–3.5%, respectively. The reflection from the front surface of the glass without anti-reflective coating reduces the short circuit current by $\sim$3.5%.

Acknowledgments

The CdTe photovoltaics program at CIE-UNAM is partially supported by the Projects SENER-CONACyT 117891, and ICyTDF. The study is also supported by the State Foundation for Fundamental Investigations of Ukraine within the Agreement Φ40.7/014.

References

[1] 〈//www.firstsolar.com/en/modules.php〉.
[2] J. Britt, C. Ferekides, Thin-film CdS/CdTe solar cell with 15.8% efficiency, Applied Physics Letters 62 (1993) 2851–2853.
[3] P.V. Meyers, S.P. Albright, Photovoltaic materials, history, status and outlook, Progress in Photovoltaics: Research and Applications 8 (2000) 161–168.
[4] D. Bonnet, CdTe thin-film PV modules, in: T. Makkvart, L. Castaner (Eds.), Practical Handbook of Photovoltaic: Fundamentals and Applications, Elsevier, Oxford, 2003, pp. 333–366.
[5] R.A. Synowicki, Spectroscopic ellipsometry characterization of indium tin oxide film microstructure and optical constants, Thin Solid Films 313–314 (1998) 394–397.
[6] D.H. Rose, F.S. Hasoon, R.G. Dhere, D.S. Albin, R.M. Ribelin, X.S. Li, Y. Mahathongdy, T.A. Gessert, P. Sheldon, Fabrication procedures and process sensitivities for CdS/CdTe solar cells, Progress in Photovoltaics: Research and Applications 7 (1999) 331–340.
[7] M.D. Archbold, D.P. Halliday. Novel tubular geometry CdTe/CdS devices, in: Record of the 33rd IEEE Photovoltaic Specialists Conference, 2008, ISSN: 0160-8371, 2009, pp. 1–4.
[8] T.S. Moss, G.J. Burrel, D. Ellis, Semiconductor Opto-Electronics, Butterworth Publishers, New York, 1973, pp. 12–17.
[9] S.O. Kasap, Optoelectronics and Photonics: Principles and Practice, Prentice Hall, New Jersey, 2000, p. 45.
[10] 〈//homepages.rpi.edu/∼schubert/Educational-resources/Materials-Refractive-index-and-extinction-coefficient.pdf〉 (E.F. Fred Schubert, Educational Resources. Refractive index and Extinction Coefficient of Materials, Rensselaer Polytechnic Institute, NY, USA, 2004).
[11] 〈//refractiveindex.info/?group=CRYSTALS&material=ITO〉.
[12] A. Compaan, R. Collins, V. Karpov, D. Giolando, Fabrication and Physics of CdTe Devices by Sputtering, Annual Technical Report, Contract no. RXL-5-44205-01, The University of Toledo, June 1, 2006–May 31, 2007, pp. 1–87.
[13] S. Ninomiya, Sadao Adachi, Optical properties of wurtzite CdS, Journal of Applied Physics 78 (1995) 1183–1190.
[14] P.D. Paulson, X. Mathew, Spectroscopic ellipsometry investigation of optical and interface properties of CdTe films deposited on metal foils, Solar Energy Materials & Solar Cells 82 (2004) 279–290.
[15] Reference Solar Spectral Irradiance at the Ground at Different Receiving Conditions, Standard of International Organization for Standardization ISO 9845-1, 1992.
[16] D. Bonnet, Cadmium telluride solar cells, in: M.D. Archer, R. Hill (Eds.), Clean Electricity from Photovoltaics, Imperial College Press, New York, 2001, pp. 245–275.
[17] Xuanzhi Wu, High-efficiency polycrystalline CdTe thin-film solar cells, Solar Energy 77 (2004) 803–814.
[18] C.S. Ferekides, U. Balasubramanian, R. Mamazza, V. Viswanathan, H. Zhao, D.L. Morel, CdTe thin film solar cells: device and technology issues, Solar Energy 77 (2004) 823–830.
[19] E.W. Jones, V. Barrioz, S.J.C. Irvine, D. Lamb, Towards ultra-thin CdTe solar cells using MOCVD, Thin Solid Films 517 (2009) 2226–2230.
[20] 〈//www.targray.com/solar/thin-film-materials/solar-glass.php〉.
[21] J.I. Pankove, Optical Processes in Semiconductors, Prentice-Hall, New Jersey, 1971, pp. 105–106.
[22] M. Born, E. Wolf, A.B. Bhatia, Principles of Optics, 7th edition, Cambridge University Press, 1999 (p. 362).